

Annealing effects on properties of LaB₆/ATO thin films deposited by magnetron sputtering

Wei Wang, Yifei Yuan, Lin Zhang, Guanghui Min *

Key Laboratory for Liquid–Solid Structural Evolution and Processing of Materials (Ministry of Education), Shandong University, Jinan 250061, China

Received 30 October 2011; received in revised form 5 February 2012; accepted 5 February 2012

Available online 14 February 2012

Abstract

A series of LaB₆/ATO films were deposited by magnetron sputtering at room temperature with the same deposition parameters. After deposition, the films were annealed at 400 °C, 700 °C and 1000 °C, respectively. The structure, morphology and opto-electrical characteristics of films were studied. It was found that the temperature for primary nucleation of LaB₆ films was about 700 °C. The crystallinity and transmissivity increased with increasing annealing temperature. After annealing at 1000 °C, the films exhibited a much higher transmissivity in the visible region than in the near-infrared area. However, the resistivity increased by one order of magnitude after heat treatment and the films without annealing presented the best electrical property.

© 2012 Elsevier Ltd and Techna Group S.r.l. All rights reserved.

Keywords: A. Films; C. Optical properties; Magnetron sputtering

1. Introduction

LaB₆ was a kind of functional ceramic materials widely used in many fields, such as high-energy optical systems, electron lithography, and coatings for resistors [1]. The structures and properties of kinds of LaB₆ samples were studied. Xu studied the impact of deposition parameters on structure and deposition rate of LaB₆ films on glass substrates [2]. Recently, the optical speciality of LaB₆ had drawn a lot of interest for its application in near-infrared (NIR) blocking [3,4].

Tin oxide (SnO₂) thin films were promising materials due to their good physical properties such as high electrical conductivity [5]. F-doped SnO₂ (FTO), Sb-doped SnO₂ (ATO) conducting thin films not only had high transparency in the visible region but also had high reflectance in the IR region [6,7]. Thin films were deposited by various methods, such as spray technique [8,9], sol–gel method [10] and RF magnetron sputtering [11]. Among these methods, magnetron sputtering had the advantage of being able to deposit high quality films at low temperatures and was readily transformable to industry for large area deposition.

Therefore, LaB₆/ATO films deposited on quartz substrates by magnetron sputtering were expected to have high transmissivity, good electricity, non-toxicity and good stability in environment. And it was interesting to combine the optical properties of LaB₆ and ATO in the NIR region. It meant that if windows were made of the glass coated by LaB₆/ATO thin films, the NIR passing through could be obviously reduced due to LaB₆'s absorption and ATO's reflection. And the outside layer ATO film could also keep the inside LaB₆ film from being oxidized. In this paper, we prepared LaB₆ films by direct-current (DC) magnetron sputtering first and then ATO films were deposited by radio-frequency (RF) magnetron sputtering on top of LaB₆ films. After that, we applied different detecting means to study the effect of annealing temperature on the films' properties.

2. Experimental

LaB₆/ATO films were deposited in a magnetron sputtering system on quartz substrates without intentional heating. The ATO target was a sintered ceramic disc (Ø 60 mm, SnO₂/Sb₂O₃ = 96:4 mol.%) with 99.99% purity, and LaB₆ target was with the same size, obtained using self-made powders in our laboratory [12]. The distance between the target and the substrate was 60 mm. The chamber was pumped down to a base

* Corresponding author. Tel.: +86 531 88395639; fax: +86 531 88395639.

E-mail address: ghmin@sdu.edu.cn (G. Min).

pressure of 5.5×10^{-4} Pa, and quartz substrates were ultrasonically cleaned in acetone and absolute EtOH alternately, both two targets were pre-sputtered for about 10 min to remove the surface oxides. During the deposition of LaB₆ films, high purity Ar (99.999%) was introduced through a mass flow controller and the sputtering pressure was 1.0 Pa. The Ar flow was 25 sccm and sputtering time was 30 min. The sputtering power was 44 W. After LaB₆ layer was prepared, the shutter would turn to confronting ATO target, and the whole deposition process was controlled by computer. For preparation of ATO films, the sputtering was carried out at a pressure of 1.5 Pa in pure argon atmosphere (99.999%) and RF power was kept at 100 W, the flow of pure argon was 25 sccm and the time lasted 10 min. After the samples were prepared, they were annealed at a thermal annealing furnace at 400 °C, 700 °C and 1000 °C, respectively, for 2 h in the air. Annealing in oxygen encouraged the further reaction between O₂ and ATO films [5], which could improve the crystallinity of the films. And LaB₆ had high oxidation resistant ability before 1273 K [13]. So the samples were annealed in air.

Crystallinity of the films was examined by the X-ray diffraction (XRD) technique (Rigaku, Japan). The optical and electrical properties were obtained by a Hall Effect Measurement System (HMS-3000, Ecopia) and a UV–Vis Spectrophotometer (U-4100, Hitachi, Japan). In order to eliminate the influences of substrates to transmittance, the optical measurement was surveyed with reference to quartz glass. The surface morphology and the fracture surfaces' morphology were investigated using an atomic force microscopy (AFM-IIa, Opto-electronics Research Institute of Zhejiang University) and a high resolution FESEM (3 kV/23 μ A, Su-70 Hitachi, Japan).

3. Results and discussion

The XRD patterns of LaB₆/ATO thin films before and after heat treatment were shown in Fig. 1(a) and (b). The XRD results indicated that the films deposited at room temperature were amorphous, and their crystallization occurred after being annealed at 400 °C. However, only very weak peaks of cassiterite SnO₂ appeared. Obvious peaks of cassiterite SnO₂ appeared after being annealed at 700 °C, which indicated that

Table 1

Grain sizes and strain values of ATO films annealed at different temperatures (Ta); negative value means compressive strain, positive value means tensile strain.

Ta (°C)	D (Å)	$\varepsilon \times 10^{-2}$
400	162	−0.317
700	188	0.728
1000	375	1.42

Table 2

Grain size and strain value of LaB₆ film annealed at 1000 °C (Ta).

Ta (°C)	D (Å)	$\varepsilon \times 10^{-2}$
1000	334	1.06

higher annealing temperature led to higher crystallinity of films. Also a weak (1 1 0) peak proved the existence of crystalline LaB₆ after the films were annealed at 700 °C. When the heat-treatment temperature increased to 1000 °C, both strong cassiterite and LaB₆ peaks appeared. However, the cassiterite peaks weakened. This was attributed to ATO thin films' thermo-dynamically unstable performance at high temperature [14]. Other peaks indicating the introduction of oxides of LaB₆ also came out. In the research carried out by Craciun [15], LaB₆ crystalline films could only be grown when substrate temperatures were higher than 800 °C. Wang applied an annealing temperature of 400 °C, failing to realize the crystallization of LaB₆ [16]. It meant that amorphous LaB₆ films needed high energy to destroy the short-range order and then crystallize, which resulted in high crystallization temperature of LaB_{6,o}.

The particle sizes of the crystalline films were calculated using the Scherer equation as follows:

$$D = \frac{0.9\lambda}{\beta \cos \theta}$$

The strain ε was also calculated according to the XRD results [17] and the values of D and ε were presented in Tables 1 and 2, respectively.

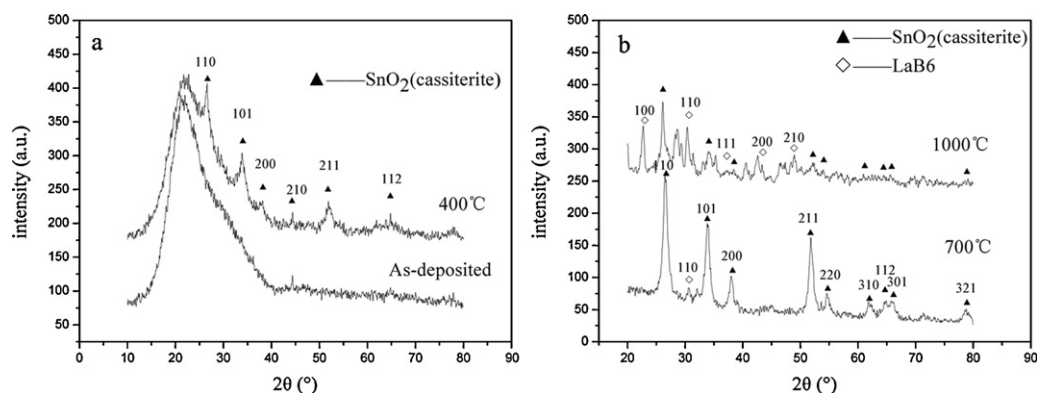


Fig. 1. XRD patterns of the thin films before and after annealing at different temperatures: (a) as-deposited and at 400 °C, (b) 700 °C and 1000 °C.

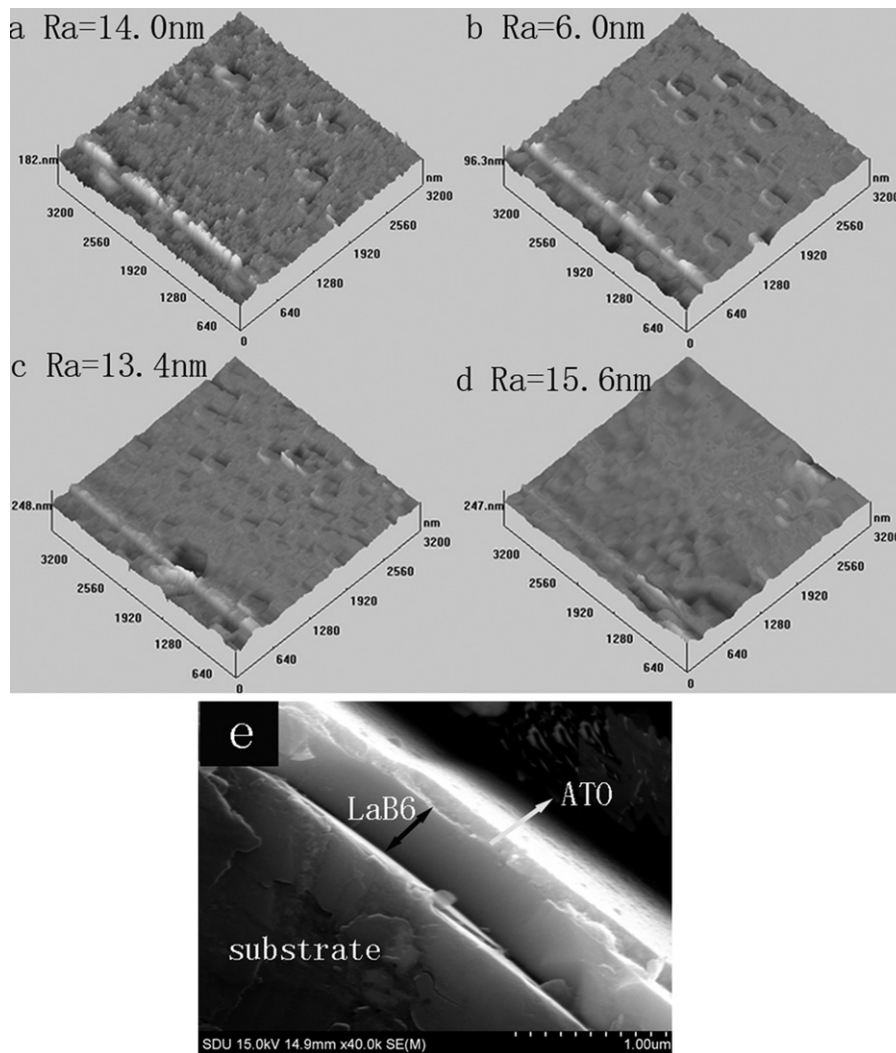


Fig. 2. AFM images of the thin films before and after annealing at different temperatures: (a) as-deposited, (b) 400 °C, (c) 700 °C, (d) 1000 °C. FESEM image of the fracture cross-sections of LaB₆/ATO films before annealing: (e).

Fig. 2(a–d) showed the surface morphology of LaB₆/ATO layers deposited on quartz substrates before and after heat treatment. The scanned area was 3.2 nm × 3.2 nm, and Ra (average roughness) value was presented. Before the heat treatment, a smooth surface was exhibited with no evident defects such as crack or bend. This also indicated that the adhesion between the films and quartz substrates was good [18]. The thickness of LaB₆/ATO films was about 600 nm according to the cross-section images, and the thicknesses of LaB₆ films and ATO films were about 450 nm and 150 nm, respectively, which could also be seen from Fig. 2(e). The high smoothness indicated that these films were suitable for the application as electrodes in devices. After the heat processing, all surfaces typically showed the granular structure. When the films were annealed at 400 °C, Ra value decreased from 14 nm to 6 nm. After annealing temperature increased to 700 °C, Ra value increased to 13.4 nm. And when the annealing temperature further increased to 1000 °C, Ra value increased to 15.6 nm.

FESEM was used to observe the microstructure of LaB₆/ATO films before and after being annealed at different

temperatures. It could be seen from Fig. 3(a–d) that the films were dense and the particle size increased with increasing annealing temperature. It showed that the films without being annealed were composed of clusters. When the films were annealed at 400 °C, the former agglomerated particles became small grains with uniform size. With the annealing temperature increasing to 700 °C, there were both small grains and big grains. And the films annealed at 1000 °C had only big grains. This was because the annealing process provided thermal energy for crystallization, recrystallization, and growth of grains in the films [19]. The as-deposited film without annealing was amorphous and composed of clusters, making the surface rough. When the thermal energy was applied, more grain boundaries were able to form. So agglomerated particles were replaced by small well-dispersed grains and the roughness was thus decreased. With the annealing temperature increasing, higher energy was applied and accelerated the growth of the crystallized grains. The bigger size of the grains made a rougher surface. The FESEM micrographs of the LaB₆/ATO films could also well explain the varied roughness of the films annealed at different temperatures.

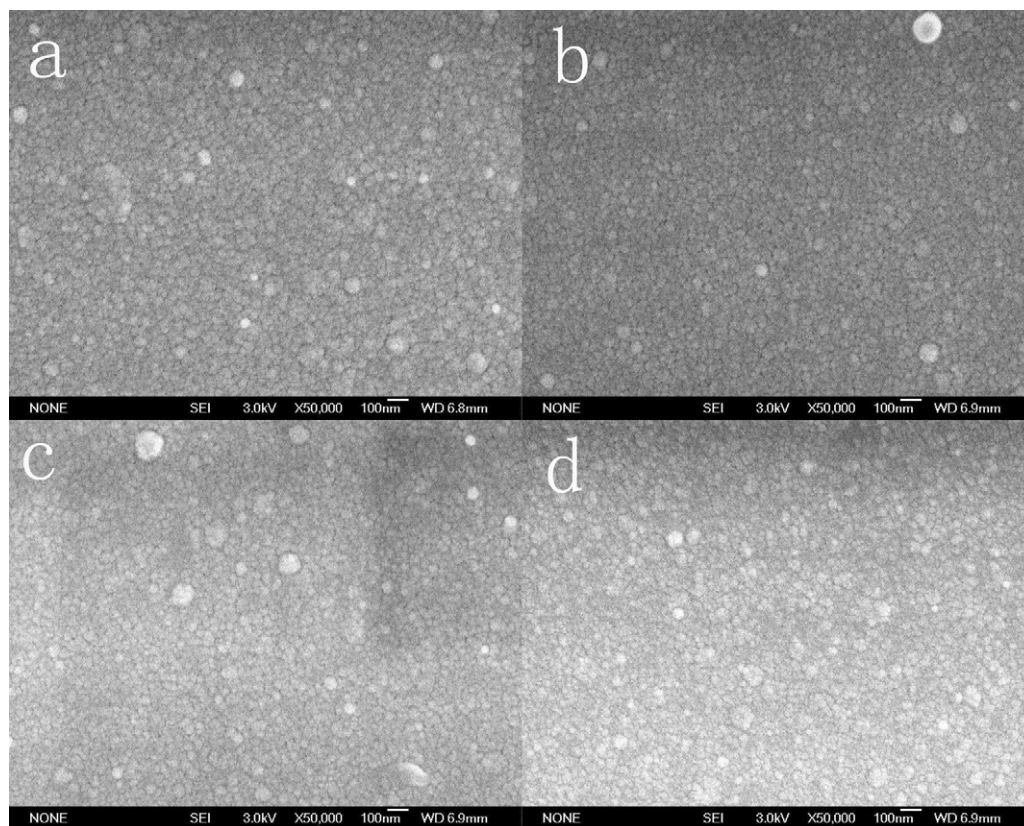


Fig. 3. FESEM images of the thin films before and after annealing at different temperatures: (a) as-deposited, (b) 400 °C, (c) 700 °C, (d) 1000 °C.

Transmittance spectrum of LaB₆/ATO films was closely related with the structure and the surface morphology. As shown in Fig. 4, the films were nearly opaque before annealing, and the transmissivity enhanced a lot after annealing. After heat treatment at 1000 °C, an interesting phenomenon occurred that the transmissivity at the infrared area was about 70%, and maximum transmissivity was about 80% at the visible area. It provided the NIR region blocking and high transmissivity in the visible region [3]. It indicated that after heat treatment at

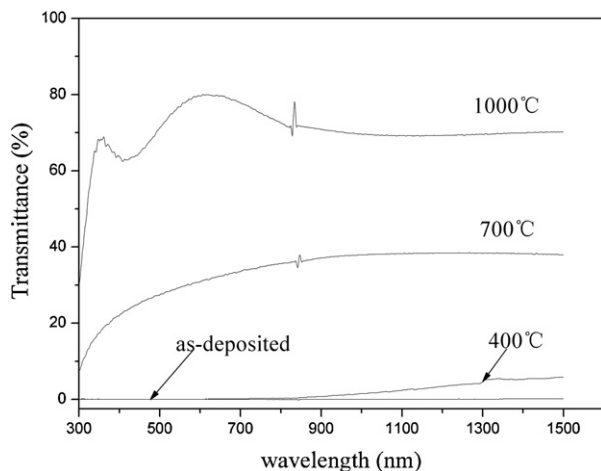


Fig. 4. Transmittance spectrum of the sputtered LaB₆/ATO films before and after annealing at different temperatures.

1000 °C, the LaB₆/ATO films' performance in optical properties was a combination of the advantages existing in both LaB₆ and ATO. According to the XRD patterns shown in Fig. 1, the films with an amorphous structure were totally opaque. This was because when the films were amorphous, the atoms prented out-of-order and short-range-order state, the scattering of light was serious [20]. Then the increase of the transmittance might be due to decreasing optical scattering caused by the densification of grains followed by grain growth and the reduction of grain boundary density. It was found by Steinhäuser [21] that when the doping level was light and the grain size was smaller than 600 nm, the grain boundary scattering mechanism was predominant. It was effective to reduce light scattering by improving the crystallinity of the films. And when the film was heavily doped and the grain size was bigger than 600 nm, the grain boundary density would have little influence on film's ability to scatter the light. Then improvements of the grain bulk quality were much more effective to reduce the light scattering. Our results were consistent with this study. Although the film's surface roughness increased with increasing annealing temperature, the films crystallized much better and the transmissivity of the films was further enhanced. But the increase was confined with the amorphous structure of the LaB₆ films at the temperature, which revealed that the structure of LaB₆ film played an important role in the optical properties of LaB₆/ATO films. When the annealing temperature reached 1000 °C, the LaB₆ films became crystalization, so the optical properties were

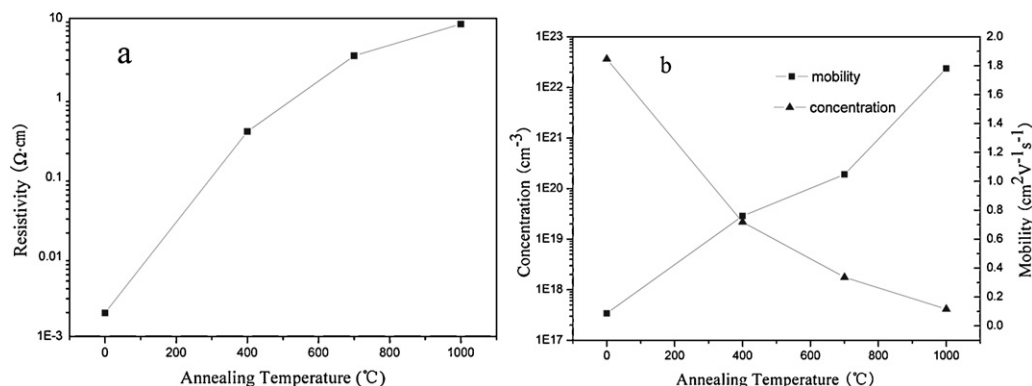


Fig. 5. (a) Resistivity vs. annealing temperature, and (b) concentration and carrier mobility vs. annealing temperature.

improved much better and it presented higher transmissivity in the visible area than in the near infrared region.

The effect of annealing temperature on the resistivity, carrier concentration and mobility was shown in Fig. 5(a) and (b), respectively. It could be seen that the resistivity rose with the increasing annealing temperature. The mobility increased with the increase of annealing temperature while the carrier concentration decreased. The resistivity was closely related with the carrier concentration and its mobility. The poor crystallization, smaller grain size with more defects led to the grain boundary scattering which reduced the carrier mobility [5,22]. With the increase of annealing temperature, the crystallinity of the films was higher, reducing the defects and the boundary scattering, so the carrier mobility increased. But the variation in the resistivity of the thin films was mainly related to the quick variation of oxygen vacancies [23]. It meant that with the increase of annealing temperature, the oxides of LaB_6 formed, which in turn made the oxygen vacancies reduced sharply, so the oxygen vacancies decreased quickly. In this way, the sharp decrease of carrier concentration and the gradual increase of the carrier mobility caused the increase of the resistivity of the films. The phenomenon that samples annealed at higher temperature showed a smaller carrier concentration and a larger resistivity is similar to the results for ATO films reported by Ni [24] and ATO particles reported by Jeon [25].

4. Conclusions

LaB_6/ATO films deposited by direct current and radio frequency magnetron sputtering method annealed at different temperatures were studied. And the relationship between the structure and the optical properties of the LaB_6 films was first studied. After the heat treatment, the amorphous films transformed to the polycrystalline state, the films' transmittance improved a lot. After being annealed at 1000 $^{\circ}\text{C}$, the thin films presented optimal optical property with a transmittance of $\sim 70\%$ in the NIR range but a much higher transmittance of $\sim 80\%$ in the visible region, which could meet the requirement of NIR blocking. However, the optimal conductive property was obtained without heat treatment with a resistivity of $1.98 \times 10^{-3} \Omega\text{-cm}$. The study, therefore, revealed that high

annealing temperature could enhance the transmittance of the LaB_6/ATO films, but increase the resistance of the LaB_6/ATO films.

Acknowledgement

This research was supported by Key Project of Natural Science Foundation of Shandong Province China (No. Z2007F09) and National Science Foundation of China (No. 51102154).

References

- [1] T. Kajiwar, T. Urakabe, K. Sano, K. Fukuyama, K. Watanabe, S. Baba, T. Nakano, A. Kinbara, Mechanical and electrical properties of rf sputtered LaB_6 thin films on glass substrates, *Vacuum* 41 (1990) 1224–1228.
- [2] J. Xu, G. Min, L. Hu, X. Zhao, H. Yu, Dependence of characteristics of LaB_6 films on DC magnetron sputtering power, *Trans. Nonferrous Met. Soc. China* 19 (2009) 952–955.
- [3] S. Schelm, G.B. Smith, Dilute LaB_6 nanoparticles in polymer as optimized clear solar control glazing, *Appl. Phys. Lett.* 82 (2003) 4346–4348.
- [4] S. Schelm, G.B. Smith, Tuning the surface plasmon resonance in nanoparticles for glazing applications, *J. Appl. Phys.* 97 (2005) 124314-1–124314-8.
- [5] J.L. Huang, Y. Pan, J.Y. Chang, B.S. Yao, Annealing effects on properties of antimony tin oxide thin films deposited by R.F. magnetron reactive sputtering, *Surf. Coat. Technol.* 184 (2004) 188–193.
- [6] C. Goebbert, R. Nonninger, M.A. Aegerter, H. Schmidt, Wet chemical deposition of ATO and ITO coatings using crystalline nanoparticles redispersable in solutions, *Thin Solid Films* 351 (1999) 79–84.
- [7] C. Terrier, J.P. Chatelon, J.A. Roger, Electrical and optical properties of Sb: SnO_2 thin films obtained by the sol–gel method, *Thin Solid Films* 295 (1997) 95–100.
- [8] K. Ravichandran, P. Philominathan, Fabrication of antimony doped tin oxide (ATO) films by an inexpensive, simplified spray technique using perfume atomizer, *Mater. Lett.* 62 (2008) 2980–2983.
- [9] B. Zhang, Y. Tian, J.X. Zhang, W. Cai, The FTIR studies of SnO_2 :Sb(ATO) films deposited by spray pyrolysis, *Mater. Lett.* 65 (2011) 1204–1206.
- [10] X.C. Chen, Synthesis and characterization of ATO/ SiO_2 nanocomposite coating obtained by sol–gel method, *Mater. Lett.* 59 (2005) 1239–1242.
- [11] J. Ni, X. Zhao, X. Zheng, J. Zhao, B. Liu, Electrical, structural, photoluminescence and optical properties of p-type conducting, antimony-doped SnO_2 thin films, *Acta Mater.* 57 (2008) 278–285.

- [12] Y. Yuan, L. Zhang, L. Liang, K. He, R. Liu, G. Min, A solid-state reaction route to prepare LaB_6 nanocrystals in vacuum, *Ceram. Int.* 37 (2011) 2891–2896.
- [13] S. Zheng, G. Min, Z. Zou, H. Yu, J. Han, W. Wang, Oxidation process of lanthanum hexaboride ceramics, *Rare Metals* 21 (2002) 101–105.
- [14] L. Cui, H.Y. Zhang, G.G. Wang, F.X. Yang, X.P. Kuang, R. Sun, J.C. Han, Effect of annealing temperature and annealing atmosphere on the structure and optical properties of ZnO thin films on sapphire (0 0 0 1) substrates by magnetron sputtering, *Appl. Surf. Sci.* (2011), doi:10.1016/j.apsusc.2011.10.076.
- [15] V. Craciun, D. Craciun, Pulsed laser deposition of crystalline LaB_6 thin films, *Appl. Surf. Sci.* 247 (2005) 384–389.
- [16] D. Wang, L. Zhang, G. Min, H. Yu, Y. Yuan, Effect of heat treatment on the properties of dc magnetron sputtered LaB_6/ITO films, *Appl. Surf. Sci.* 257 (2011) 6418–6423.
- [17] N.S. Ramgir, Y.K. Hwang, I.S. Mulla, J.S. Chang, Effect of particle size and strain in nanocrystalline SnO_2 according to doping concentration of ruthenium, *Solid State Sci.* 8 (2006) 359–362.
- [18] S.Y. Tsai, Y.M. Lu, M.H. Hon, Comparison with electrical and optical properties of zinc oxide films deposited on the glass and PET substrates, *Surf. Coat. Technol.* 200 (2006) 3241–3244.
- [19] V. Senthilkumar, P. Vickraman, J. Joseph Prince, M. Jayachandran, C. Sanjeeviraja, Effects of annealing temperature on structural, optical, and electrical properties of antimony-doped tin oxide thin films, *Philos. Mag. Lett.* 90 (2010) 337–347.
- [20] S.F. Wang, Y.F. Hsu, Y.S. Lee, Microstructural evolution and optical properties of doped TiO_2 films prepared by RF magnetron sputtering, *Ceram. Int.* 32 (2006) 121–125.
- [21] J. Steinhäuser, S. Faÿ, N. Oliveira, E. Vallat-Sauvain, C. Ballif, Transition between grain boundary and intragrain scattering transport mechanisms in boron-doped zinc oxide thin films, *Appl. Phys. Lett.* 90 (2007) 142107.
- [22] Y. Seki, Y. Sawada, M.H. Wang, H. Lei, Y. Hoshi, T. Uchida, Electrical properties of tin-doped indium oxide thin films prepared by a dip coating, *Ceram. Int.* (2011), doi:10.1016/j.ceramint.2011.05.109.
- [23] Y.S. Kim, Y.C. Park, S.G. Ansari, J.Y. Lee, B.S. Lee, H.S. Shin, Influence of O_2 admixture and sputtering pressure on the properties of ITO thin films deposited on PET substrate using RF reactive magnetron sputtering, *Surf. Coat. Technol.* 173 (2003) 299–308.
- [24] J. Ni, X. Zhao, X. Zheng, J. Zhao, B. Liu, Electrical, structural, photoluminescence and optical properties of p-type conducting, antimony-doped SnO_2 thin films, *Acta Mater.* 57 (2009) 278–285.
- [25] H.J. Jeon, M. Kang, S.G. Lee, Y.L. Lee, Y.K. Hong, B.H. Choi, Synthesis and characterization of Jeon antimony-doped tin oxide (ATO) with nanometer-sized particles and their conductivities, *Mater. Lett.* 59 (2005) 1801–1810.